SCIENCE CHINA
Technological Sciences

Special Topic: Performance Analysis and Design of Critical Civil Engineering Structures under Multiple Hazards
•Article•

February 2023 Vol.66 No.2: 363–377
https://doi.org/10.1007/s11431-022-2265-5

Reliability analysis of reinforced concrete columns under combined seismic and blast loads

SHI YanChao[1,2*], SUN XiaoZhe[2] & CUI Jian[1,2]

[1] *Key Laboratory of Coast Civil Structure Safety of Ministry of Education, Tianjin University, Tianjin 300354, China;*
[2] *School of Civil Engineering, Tianjin University, Tianjin 300354, China*

Received July 29, 2022; accepted November 18, 2022; published online December 28, 2022

It is possible for certain building structures to encounter both the seismic load and blast load during their service life. With the development of the economy and the increase of security demand, the need for design of building structures against multi-hazard is becoming more and more obvious. Therefore, the damage analysis of building structures under the combined action of multiple hazards has become a very urgent requirement for disaster prevention and reduction. In this paper, the refined finite element model of reinforced concrete (RC) columns is established by using the explicit dynamic analysis software LS-DYNA. Combined with the Monte Carlo method, the damage law of RC columns under the combined action of random single earthquake or explosion disaster and multi-hazard is studied, and the damage groups are distinguished according to the damage index. Based on the support vector machine (SVM) algorithm, the dividing line between different damage degree groups is determined, and a rapid method for determining the damage degree of RC columns under the combined seismic and blast loads is proposed. Finally, suggestions for the design of RC column against multi-disaster are put forward.

reliability analysis, reinforced concrete (RC) column, damage probability, seismic load, blast load, Monte-Carlo method

Citation: Shi Y C, Sun X Z, Cui J. Reliability analysis of reinforced concrete columns under combined seismic and blast loads. Sci China Tech Sci, 2023, 66: 363–377, https://doi.org/10.1007/s11431-022-2265-5

1 Introduction

With the progress of science and technology, human society is developing at an unprecedented speed in history, but disasters caused by various reasons often bring life and property losses and affect people's normal production and life order. In recent years, terrorist attacks against civilian buildings have been reported more frequently all over the world, and explosions caused by various security accidents are also common. The blast loads from terrorists or accidental explosions often cause the destruction of structural components, which might lead to the collapse of the building structures. Serious explosion disasters are common all over the world, such as the terrorist attack on the federal building in Oklahoma in 1995, the terrorist attack on the twin towers of the world trade center on September 11, 2001, the ammonium nitrate explosion at the port of Beirut, the capital of Lebanon in 2020, and so on. At the same time, earthquakes are also common natural disasters. Earthquakes with high intensity will cause very serious damage to building structures. Strong earthquakes themselves, their aftershocks and secondary disasters such as tsunamis, floods, landslides, fire and explosions will also pose a serious threat to people's lives and property, such as the magnitude 7.3 earthquake From Kansai Osaka to Kobe in 1995, the magnitude 8.7 earthquake in Sumatra Island, Indonesia in 2004 and the magnitude 9.0 Earthquake in Northeast Japan in 2011. At the same time, the small earthquake might also cause light damage to building structures, which might reduce their blast resistant capacity during the service life. With the relevant

*Corresponding author (email: adqiao@bjut.edu.cn)

research in recent years, the research on disaster resistance for a single disaster such as an earthquake and explosion has been relatively complete, but the research on damage caused by multi-hazard is still lacking. Therefore, it is interesting to investigate the damage of building structures under combined seismic and blast loads.

In recent years, more and more scholars have studied the structural performance under multi-hazard. Considering the complexity of multiple disasters, the structural performance under multiple disasters is quantitatively studied by the probability method. The variability of each parameter is generally sorted out according to relevant tests or statistics of real cases. The main contents of the research include damage or failure risk assessment under multiple disasters, structural design suggestions and relevant methods against multiple disasters. The disasters considered include earthquakes, explosions, as well as fires, wave erosion, freezing and thawing, fatigue, shocks, gusts and so on. For example, Li et al. [1] and Fascetti et al. [2] reviewed the extreme disasters in history, and drew the conclusion that the design method for a particular hazard often had an adverse effect on the structural performance of other hazards. The design method and reliability evaluation method of structure should change from single disaster protection to multi-disaster comprehensive consideration. Lin et al. [3] believed that there are obvious differences between the seismic design of structures and the design of anti-progressive collapse. The focus of the seismic design is to resist lateral seismic forces, while the design of anti-progressive collapse is to resist vertical loads caused by local destruction. In order to meet the requirements of seismic and progressive collapse resistant design of structures, a new multi-disaster precast concrete (MHRPC) frame is proposed and the multi-disaster design requirements of MHRPC frame system against earthquake and progressive collapse are verified by test and numerical simulations. Abdollahzadeh and Faghihmaleki [4–6] proposed a new method to evaluate the robustness index of RC frame under the risk of joint occurrence of earthquake and explosion. By analyzing the ratio of current force to ultimate bearing capacity (DCR) of shear or moment, the probability of progressive collapse in each scene was studied, and the failure curve of RC column was plotted to measure the risk of structural collapse. Using this robustness evaluation method, Abdollahzadeh and Faghihmaleki [7] evaluated the annual progressive collapse probability for the seismic designed frame located in the seismic susceptible area under simultaneous seismic and explosive loads. Feng et al. [8] proposed a method to calculate the robustness of frame structure based on probability density evolution method (PDEM). The static non-linear Pushdown method based on finite element analysis was used to analyze the capability of resisting progressive collapse. Then the PDEM method was used to calculate the probability density function of load factor and the probability and reliability of structural failure under specific disasters. Finally, robustness index was obtained by comparing the original structural reliability index with the damage reliability index. Stochino et al. [9] studied the vulnerability of reinforced concrete (RC) frame with the seismic design based on the Monte Carlo method. The simplified equivalent single-degree-of-freedom system was used to carry out non-linear displacement analysis considering the uncertainties of both the explosion distance and equivalent charge weight. It was found that the seismic design is beneficial in improving the blast resistance of the structure. Elhami Khorasani et al. [10] established a program to evaluate the reliability of structures in post-earthquake fire (FFE) and applied it to of a nine-storey steel bending moment frame as an example. The program considered uncertainties of both the high temperature and material properties.

Based on the relevant theory and experimental research of RC column members, the dynamic response of RC columns under combined seismic and blast loads are simulated through MATLAB and LS-DYNA. Firstly, the finite element model is established and verified by simulating relevant explosion tests and seismic tests, and then used to study the effectiveness of blast and seismic action on structural responses. The damage probability of RC column under blast load and seismic load are studied considering the uncertainties of blast load, seismic load and member resistance. The probability distribution of damage of the RC column under combined blast and seismic load is analyzed based on Monte Carlo method. A method to determine the damage degree of RC columns under the combined action of blast and seismic load is proposed. By defining different damage degree indexes of RC columns, the damage degrees of RC column under different blast and seismic loads are grouped, and the boundary of different damage groups is determined based on the support vector machine (SVM) algorithm and the analytical formula of boundary for any RC column member is derived.

2 Establishment of finite element model

2.1 Modeling methodology

In this paper, a segregated model is used to simulate the dynamic response of RC columns under seismic and blast loads by dividing the grid and endowing the material with a finite element model of steel bar and concrete as different units in consideration of operational accuracy and time. At the longitudinal ends of the separated model, the rigid column head and foot are established respectively, and all degrees of freedom except the vertical displacement of the column head are restrained to reproduce the boundary conditions of the RC columns.

When establishing the finite element model of RC column, the beam element is used to model the reinforcement, the solid element is used to model the concrete, the column head, the column foot and the air material. Through the convergence analysis of the mesh size, the mesh size of reinforcement, concrete, the column head and the column foot is chosen to be 20 mm, and the mesh size of air is 50 mm. When choosing this mesh size, both the computational efficiency and the accuracy of the results can be considered.

It should be noted here that a perfect bond between concrete and steel bars is assumed. Neglecting the bond slip behavior between steel reinforcement and concrete would lead to the error in the dynamic response of RC column under both seismic and blast loads. However, the error is acceptable since it only affects the dynamic response of the RC column at the unloading stage. At the same time, numerical simulation of bond slip behavior between steel reinforcement and concrete is very time consuming, therefore it is no suitable for Monte Carlo simulations which require large amount of numerical simulations.

2.2 Material model

2.2.1 Concrete material model

The main materials for RC column include concrete material, steel reinforcement material, and air material. For concrete, considering the strain rate effect, large deformation effect, cumulative damage and other characteristics that may occur in an earthquake or explosion, the K&C model is chosen for concrete materials, i.e., the MAT072R3 model in the LS-DYNA material library, and the MAT072R3 model is an improved version of MAT072 [11], which can be simplified to achieve the effect of MAT072 materials [12,13]. The K&C model is commonly used in the numerical analysis of RC structures under blast loads and has been proved to be good. In this paper, the same concrete material models are used to simulate the damage and failure of reinforced concrete columns under seismic and blast loads.

Under blast loading, concrete materials may reach strain rates of 10 to 1000 s^{-1} [14], and at high strain rates, the concrete material strength may be increased due to the strain rate effect. And the concrete compressive strength may be increased by up to 100% and the tensile strength by up to 600% [15], so the strain rate effect on the concrete material strength needs to be considered. The strain rate effect of the material can be expressed by the dynamic increase factor (DIF) of the material strength, which is the ratio of the actual strength of the material at a given strain rate to its nominal strength under static forces as eq. (1).

$$\mathrm{DIF}=\frac{f_d}{f_s}. \tag{1}$$

The compressive strength dynamic amplification factor CDIF for the K&C model for concrete materials is determined by eqs. (2)–(4) [16].

$$\mathrm{CDIF}=\frac{f_{cd}}{f_{cs}}=\begin{cases}\left(\dfrac{\dot{\varepsilon}}{\dot{\varepsilon}_s}\right)^{1.026\alpha}, & \dot{\varepsilon}\leqslant 30\ \mathrm{s}^{-1},\\ \gamma_s\left(\dfrac{\dot{\varepsilon}}{\dot{\varepsilon}_s}\right)^{1/3}, & \dot{\varepsilon}>30\ \mathrm{s}^{-1},\end{cases} \tag{2}$$

$$\lg\gamma_s=6.156\alpha-2, \tag{3}$$

$$\alpha=1/\left(5+9f_{cs}/f_{c0}\right), \tag{4}$$

where $\dot{\varepsilon}_s$ is taken as 30×10^{-6} s^{-1}; f_{c0} is taken as 10 MPa.

The tensile strength dynamic amplification factor TDIF is determined by eqs. (5)–(7) [14,17].

$$\mathrm{TDIF}=\frac{f_{td}}{f_{ts}}=\begin{cases}\left(\dfrac{\dot{\varepsilon}}{\dot{\varepsilon}_s}\right)^{\delta}, & \dot{\varepsilon}\leqslant 1\ \mathrm{s}^{-1},\\ \beta_s\left(\dfrac{\dot{\varepsilon}}{\dot{\varepsilon}_s}\right)^{1/3}, & \dot{\varepsilon}>1\ \mathrm{s}^{-1},\end{cases} \tag{5}$$

$$\lg\beta_s=6\delta-2, \tag{6}$$

$$\delta=1/\left(1+8f_{ts}/f_{t0}\right), \tag{7}$$

where $\dot{\varepsilon}_s$ is taken as 10^{-6} s^{-1}; f_{t0} is taken as 10 MPa.

2.2.2 Steel bar material model

The steel material is chosen to be simulated in a bifold model, i.e., MAT003 model. The strain rate effect of the steel material is considered and the steel reinforcement material dynamic amplification factor DIF is expressed using the Cowper & Symonds model as eq. (8) [18–21].

$$\mathrm{DIF}=1+\left(\frac{\dot{\varepsilon}}{c}\right)^{1/p}, \tag{8}$$

where c is taken as 5.0 s^{-1} and p is taken as 40.0 s^{-1}.

2.2.3 Air material model

In simulating the blast action, this paper uses a fluid-solid coupling approach to apply the blast load, which requires the simulation of air domain. Air can be considered as an ideal non-viscous gas, therefore the MAT009 model is chosen for the air material and the air material equation of state is determined by eqs. (9) and (10).

$$p=c_0+c_1\mu+c_2\mu^2+c_3\mu^3+\left(c_4+c_5\mu+c_6\mu^2\right)E_0, \tag{9}$$

$$\mu=\frac{1}{v_0}-1, \tag{10}$$

where E_0 is the initial internal energy per unit volume, taken as 2.5×10^5; c_0 to c_6 are coefficients related to the thermodynamic properties of air, where c_4 and c_5 are taken as 0.4, and the rest of the coefficients are taken as 0; v_0 is taken as 1.0.

2.3 Validation of finite element model

In this section, the seismic action is approximately simulated

by transforming the seismic response of the structure into the displacement spectrum and applying horizontal displacement to the column base in the finite element model. The blast load is directly applied on the front face of the RC column through keyword Load-Blast-Enhanced in LS-DYNA, and the air layer is established in the finite element model to ensure more accurate simulation effect.

2.3.1 Validation of finite element models under seismic loads

In general, the seismic performance analysis methods applicable to RC columns include the time-step analysis method and the static method. The time-step analysis method usually inputs amplitude-modulated real or artificial seismic waves in the simulation process. The static method usually obtains the seismic capacity of the structural member by applying cyclic loads by force control criterion or displacement control criterion.

To verify the applicability of the finite element model, the numerical model was used to simulate the test results of the static test RC-0 column specimen by Qiu et al. [22]. The dimensions of the RC-0 column are shown in Figure 1. As can be seen, the RC column is reinforced with longitudinal reinforcement 8Φ12, hoop reinforcement Φ6@50, and the concrete strength f_c=39.6 MPa, axial compression ratio equals 0.228. The test was performed using the displacement control loading strategywith 3 cycles for each loading stage, and the displacement increment for each stage is 5 mm.

The comparison between the finite element simulation results and the experimental results is shown in Figure 2. It can be seen that the hysteresis curve and skeleton curve obtained from the finite element simulation are closer to the experimental results, and it can be concluded that the finite element model can better reflect the dynamic response and damage mode of the RC column under seismic loads.

2.3.2 Validation of finite element models under blast loads

In LS-DYNA, a variety of different blast action simulation

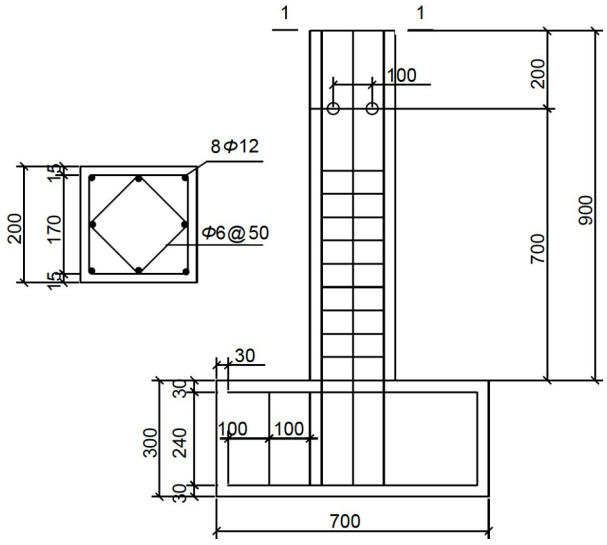

Figure 1 RC-0 column specimen size and reinforcement diagram.

methods can be used [23–25], including the fluid-solid coupling method (ALE), the semi-empirical simulation method (LBE), and the direct loading method (LSS). Considering that the conditions of this study are dominated by medium- and long-range explosions, the LBE method, which is applicable to medium- and long-range explosions and has higher accuracy, is selected to simulate the effects of RC column members under the blast loads.

To verify the applicability of the finite element model, the above model was used to simulate Woodson & Baylot [26,27] test No. 2. A schematic diagram of Woodson & Baylot's test specimen No. 2 is given in Figure 3, and the explosion parameters of the test are shown in Table 1, the geometric parameters of the target column are shown in Table 2, and the material parameters are shown in Table 3.

In the numerical simulation process, the initial axial pressure was first slowly applied to the top of the column with a value of 2.1 MPa, and after the vertical static force equilibrium, the explosion process was simulated. The comparison between the finite element simulation results and

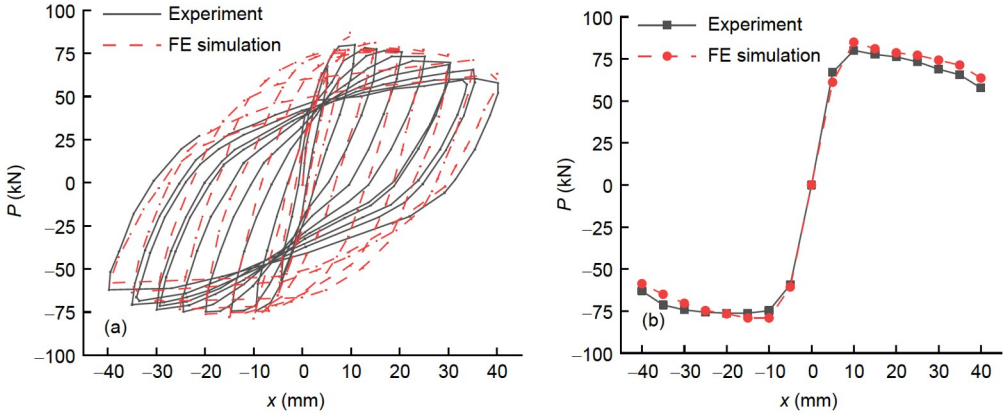

Figure 2 (Color online) Comparison of hysteresis curves (a) and skeleton curves (b) between FE simulation and experimental results.

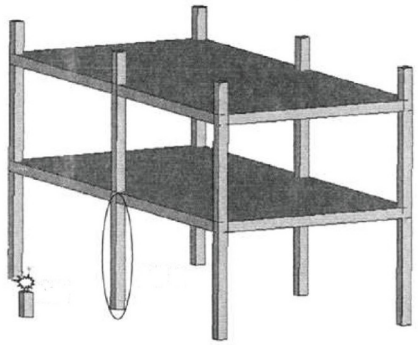

Figure 3 Schematic diagram of test specimen No. 2 of Woodson & Baylot experiment.

Table 1 Explosion parameters of the test

Quality of C4 explosives (kg)	Equivalent TNT mass (kg)	Distance (mm)	Height of explosives (mm)	Initial axial stress (MPa)
7.1	8	1070	229	2.1

Table 2 Geometric parameters of the target column

b (mm)	h (mm)	H (mm)	Hoop reinforcement	Longitudinal reinforcement	c (mm)
85	85	900	Φ1.6@100	8Φ3.2	8.5

Table 3 Material parameters of the target columns

f_c (MPa)	Longitudinal reinforcement			Hoop reinforcement		
	f_y (MPa)	f_s (MPa)	Ultimate strain (%)	f_y (MPa)	f_s (MPa)	Ultimate strain (%)
42	450	510	18	400	610	18

the test results is shown in Figure 4.

It can be seen that both the maximum and residual displacement of the RC column from FE simulation agree well with those from the experimental results. The only difference is the vibration frequency, which might be due to neglecting the bond slip behavior between steel reinforcement and concrete. What's more, the damage modes of the RC column agree with each other as well. Thus, it can be concluded that the finite element model can better simulate the dynamic response and damage mode of RC column under blast loads.

3 Parameter stochasticity of combined seismic and explosive effects

3.1 Seismic effect

The stochastic nature of ground shaking is generally considered to be influenced by a variety of factors, such as source depth, epicenter distance, seismic wave form, propagation medium, and site soil classification. It is generally

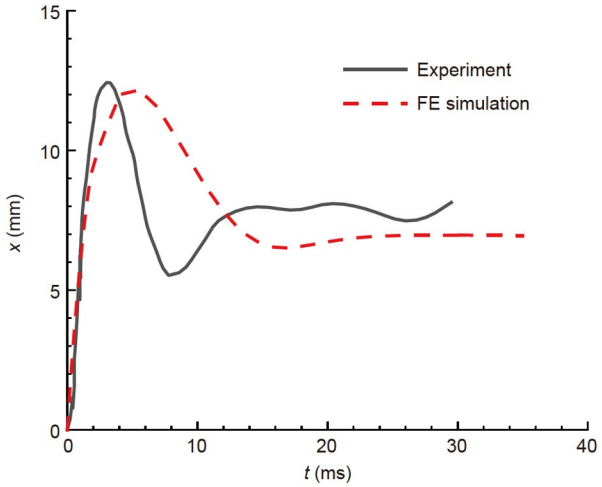

Figure 4 (Color online) Comparison of FE simulation and experimental results.

accepted that the basic properties of a given earthquake can be measured by three elements of ground shaking, including peak value, spectral characteristics, and duration. As is well known to all, the peak acceleration can be determined based on the actual intensity of the earthquake. According to the statistics of related scholars, the probability distribution of the maximum seismic intensity during the 50-year design basis period is consistent with the extreme value type III distribution as eqs. (11) and (12).

$$P_I(I) = \exp\left[-\left(\frac{12-I}{12-I_s}\right)^k\right], \tag{11}$$

$$I_s = I_0 - 1.55, \tag{12}$$

where I is the seismic intensity; $P_I(I)$ is the cumulative distribution function of seismic intensity, which conforms to the extreme value type III distribution; I_s is the multitude intensity; I_0 is the fortification intensity; k is the shape coefficient. The coefficients corresponding to different fortification intensities can be selected according to Table 4 and Figure 5.

Meanwhile, the actual intensity of an earthquake has the following relationship with the peak acceleration is determined by eq. (13).

$$A_{\max} = 10^{(I\cdot \lg 2 - 0.01)}. \tag{13}$$

In this study, the Kobe wave is selected as the acceleration of the seismic wave. And the acceleration will be adjusted by eq. (13) when required.

Table 4 Parameters of different fortification intensities

Parameter	Value			
I_0	6	7	8	9
I_S	4.45	5.45	6.45	7.45
k	9.79	8.33	6.87	5.40

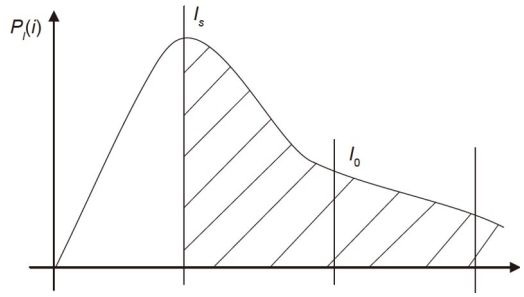

Figure 5 Schematic diagram of multitude intensity I_s and fortification intensity I_0.

3.2 Blast load

In this paper, vehicle-borne improvised explosive devices (VBIED) working condition is selected. This study considers three aspects of variability: explosive mass of the blast load, blast distance, and inherent variability.

The uncertainty of the quality of explosives mainly has two factors to determine: one is the user factor, expressed in W_{user}; the second is the explosive factor, expressed in W_{NEQ}, considering the uncertainty of explosives quality of the explosive quality calculation formula is determined by eq. (14).

$$W = W_{nom} \times W_{user} \times W_{NEQ}. \tag{14}$$

For the VBIED condition, W_{user} obeys a normal distribution with a mean value of 1 and a coefficient of variation of 0.102; W_{NEQ} obeys a triangular distribution with a probability density function with an upper bound of 1, a lower bound of 0, and a peak located at 0.82, schematically shown in Figure 6, corresponding to a mean value of 0.607 and a coefficient of variation of 0.359 [28].

The blast distance R is determined by eq. (15), where x and y both obey normal distribution with the mean being the nominal distance, the variance of x is 1.53 m, as well as the variance of y is 3.06 m [28].

$$R = \sqrt{x^2 + y^2}. \tag{15}$$

The inherent variability is the variability that arises when the person concerned reads the data and uses the test apparatus and is generally expressed as ln. The intrinsic variability ln obeys a normal distribution with a mean of 1 and a coefficient of variation of 0.01 [28].

Figure 6 Schematic diagram of WNEQ probability density function.

3.3 Geometric parameters

The geometric parameters of the components generally include the cross-sectional height and width of the components, the height and span of the components, etc. The variability is generally the deviation of the geometric dimensions of the components caused by the processes of transportation, installation and movement during the construction process, and the uncertainty of the geometric parameters is generally expressed by the random variable K_A. K_A is determined by eq. (16), as well as the relevant geometric parameters corresponding to K_A shown in Table 5 [29,30].

$$K_A = a / a_k. \tag{16}$$

3.4 Material parameters

The material parameters of the members generally include the yield strength and modulus of elasticity of the member materials, and their variability is generally influenced by the combination of the material's own differences, construction process, and environmental conditions. The uncertainty of material parameters is generally expressed by the random variable K_M. K_M is determined by eq. (17), as well as the relevant geometric parameters corresponding to K_M are shown in Table 6 [29].

$$K_M = a / a_k. \tag{17}$$

4 Damage analysis of RC column under combined seismic and explosive effects

4.1 Monte Carlo method for combined seismic and explosive processes

The Monte Carlo method (MC method) is one of the most commonly used computational methods for studying multi-hazard injuries, which consists of the following three main steps.

(1) Screening random variables and determining the distribution type and related parameters according to the computational needs.

(2) Generating the initial conditional sample set based on the random sampling method.

(3) Performing calculations on the sample set of cases, counting and processing the results of the calculations.

The structural damage probability p_F obtained based on the Monte Carlo method is determined by eq. (18).

$$p_F \approx \widehat{p}_F{}^{MCS} = \frac{1}{N}\sum_{i=1}^{N} I_F(\theta_i). \tag{18}$$

Table 5 Geometric parameters K_A statistical parameters

Geometric parameter	Mean value	Coefficient of variation	Distribution type
Column width b	1.00	0.03	Normal
Column depth h	1.00	0.03	Normal
Column height H	1.00	0.03	Normal
Thickness of protective layer c	1.00	0.145	Normal

Table 6 Material parameter K_M statistical parameters

Material parameter	Mean value	Coefficient of variation	Distribution type
Concrete compressive strength f_c	1.02	0.12	Lognormal
Yield strength of reinforcing steel f_y	1.15	0.05	Lognormal
Modulus of elasticity of reinforcement E_S	1.00	0.04	Normal

In the simulation process of the Monte Carlo method, each independent and operationally identical structural reliability analysis corresponds to eq. (18), which in turn allows for a corresponding analysis of the damage probability.

When analyzing the damage of the same structural member after experiencing blast and seismic effects, respectively, it is crucial to find common damage indicators. In related studies, the damage indicators for quantifying the calculation of blast damage or seismic damage include residual bearing capacity, ultimate deformation, cumulative energy dissipation, and so on.

Residual bearing capacity refers to the degree of residual bearing capacity of the member after suffering a disaster. For the RC column, its main residual bearing capacity index is the vertical residual bearing capacity, which has better applicability.

Therefore, in this paper the axial residual bearing capacity is utilized as a unified damage index. For column members, the damage index D is used to assess the degradation of the axial residual bearing capacity, and its calculation formula is determined by eq. (19).

$$D = 1 - \frac{P_r - P_p}{P_N - P_p}, \tag{19}$$

where P_N is the initial axial bearing capacity of RC column, P_r is the residual axial bearing capacity of RC column, and P_p is the initial axial force of RC column.

In this study, it is necessary to determine the actual blast and seismic loads. Considering that the probability of seismic and blast occurring simultaneously is very small, the seismic load and blast load are sequentially applied on the RC column. It is assumed that the earthquake occurs firstly, and if the RC column is light damage, an explosion occurs again during the service life of the building structures. That is to say, the focus of this study is on the case that the RC column firstly suffers an earthquake and then an explosion, and the subsequent analysis steps are designed accordingly. The specific Monte Carlo process is shown specifically below eqs. (1)–(6), and the flow schematic is shown in Figure 7.

(1) A sample set with n samples is generated according to the parameter variability random sampling method as the initial condition for the finite element simulation analysis.

(2) Determine the relevant conditions of seismic action and explosion action according to the initial conditions of n samples, and establish the corresponding finite element model to determine the initial bearing capacity of RC column members.

(3) Simulate the seismic action in n samples, determine the damage and statistics of the n samples after the seismic action, and generate the damage probability curve I.

(4) For the sample set of finite element model that simulates the completed seismic action, determine whether the n samples reach the damage threshold, and the samples that reach the damage threshold and are judged to be failed are counted as the failure sample set I, and then exit the calculation cycle; for the m samples that do not reach the damage threshold, simulate the effect of the secondary blast action on the RC column member by restarting the method according to the initial conditions of the samples.

(5) Simulate the completion of the explosion effect of the finite element model sample set, respectively, to determine whether the m samples reach the damage threshold, to reach the damage threshold and determine the failure of the samples are included in the failure sample set II; for the samples that do not reach the damage threshold, are included in the damaged sample set; then at this time can be generated according to the failure sample set I, failure sample set II and damaged sample set damage probability curve II.

(6) Re-simulation of n samples of the finite element model of the blast effect, according to the results of finite element simulation to generate damage probability curve III.

4.2 Sensitivity analysis of parameters

In order to compare the degree of influence of variability of

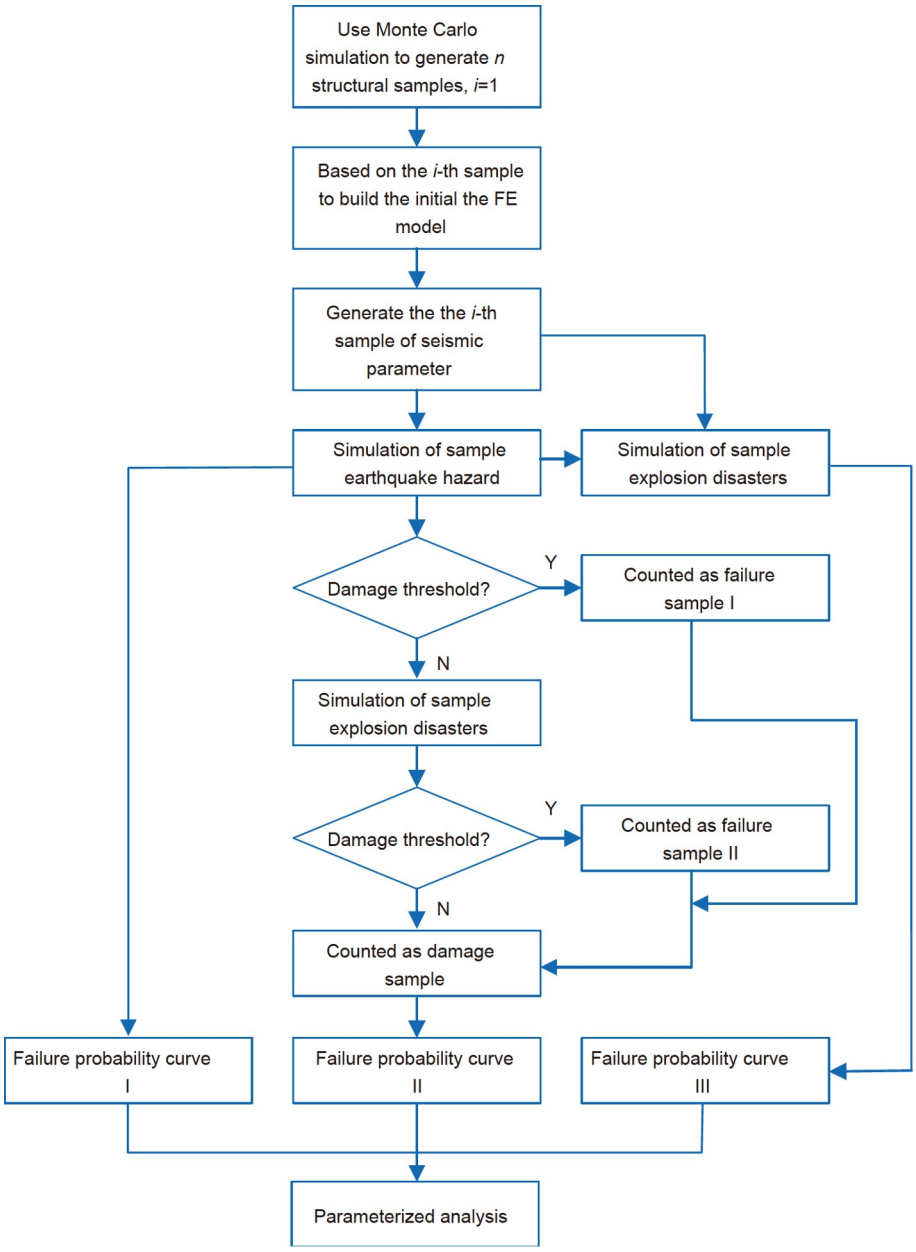

Figure 7 (Color online) Flow chart of Monte Carlo process for combined blast and seismic analysis.

different variables on the load bearing capacity of RC columns under multi-hazards, a sensitivity analysis of each random variable using tornado diagram analysis is proposed. The damage criteria of RC columns are quantified using the residual bearing capacity coefficient D. The tornado diagram analysis method is divided into the following three steps.

(1) All variables are selected as mean values and their residual bearing capacity is calculated.

(2) Taking the upper limit (mean+standard deviation) or lower limit (mean−standard deviation) for a variable and selecting the mean value for all the remaining variables to form the initial conditions of the finite element model considering the RC column damage analysis under that variable and calculating its residual bearing capacity.

(3) Calculate all variables corresponding to the residual bearing capacity, and arrange their deviation values in descending order.

The tornado diagram drawn according to the above method can visually show the degree of influence of different variables on the calculation result of the residual bearing capacity coefficient D. The longer the strip, the higher the ranking position and the more sensitive the calculation result is to the variation of this variable.

A typical RC column member is used as the object of study, and its parameters are shown in Table 7, in which there are 8 longitudinal bars with a diameter of 16 mm, hoop bars

Table 7 RC column parameters

Parameter	Value	Parameter	Value
b (mm)	400	f_c (MPa)	40
h (mm)	400	f_y (MPa)	400
H (mm)	3600	f_y (MPa)	300
c (mm)	25	E_S (GPa)	200
ρ_s	0.010		
ρ_{sv}	0.008		

with a diameter of 10 mm and spacing of 200 mm.

In the sensitivity analysis, set its working conditions for seismic intensity 7, VBIED explosion scenario under the nominal mass of explosives 1000 kg, the equivalent TNT mass of nominal mass W_{nom} is 607 kg, the explosion distance of 10 m, sensitivity analysis of the various parameters considered and their statistical parameters are shown in Table 8.

A comparison of the results obtained from the finite element simulation is shown in Table 9. The plotted tornado diagram is also shown in Figure 8.

The tornado diagram visually shows that the variability of the random parameters such as column width b, column depth h, concrete compressive strength f_c, explosion inherent variability ln, column height H, concrete protective layer thickness c, and reinforcement elastic modulus E_s has an error relative value of less than 5% on the damage index D. It can be considered that their variability has minimal impact on the final damage probability calculation. Therefore, for

Table 8 Sensitivity analysis parameters

Parameter type		Distribution type	Mean	COV/VAR	Ref.
Geometric parameters	b (mm)	Normal	400	0.03	[31]
	h (mm)	Normal	400	0.03	[31]
	H (mm)	Normal	3600	0.03	[31]
	c (mm)	Normal	25	0.145	[30]
Material parameters	f_c (MPa)	Lognormal	40.8	0.12	[29]
	f_y (MPa)	Lognormal	460	0.05	[29]
	f_{yv} (MPa)	Lognormal	345	0.05	[29]
	E_s (GPa)	Normal	200	0.04	[29]
Seismic parameters	Seismic intensity	Extreme III	5.82	0.15	[29]
	W_{NEQ}	Triangle	0.607	0.359	[28]
	W_{user}	Normal	1.000	0.102	[28]
Blast parameters	x (m)	Normal	10	σ_x=1.53 m	[28]
	y (m)	Normal	0	σ_y=3.06 m	[28]
	In	Normal	1.000	0.01	[28]

Table 9 Sensitivity analysis results

Parameter	Lower extreme		Upper extreme	
	D_m	Difference (%)	D_m	Difference (%)
W_{NEQ}	0.277	−58.36	0.816	22.75
x	0.818	23.02	0.366	−44.97
y	0.488	−26.56	0.496	−25.46
Seismic intensity	0.584	−12.24	0.847	27.27
W_{user}	0.540	−18.79	0.764	14.92
fy	0.747	12.37	0.628	−5.62
fyv	0.716	7.64	0.619	−7.01
h	0.696	4.66	0.644	−3.25
b	0.681	2.40	0.632	−4.92
fc	0.683	2.75	0.636	−4.40
H	0.650	−2.24	0.687	3.33
In	0.640	−3.84	0.665	−0.10
c	0.654	−1.72	0.674	1.32
Es	0.675	1.55	0.661	−0.61

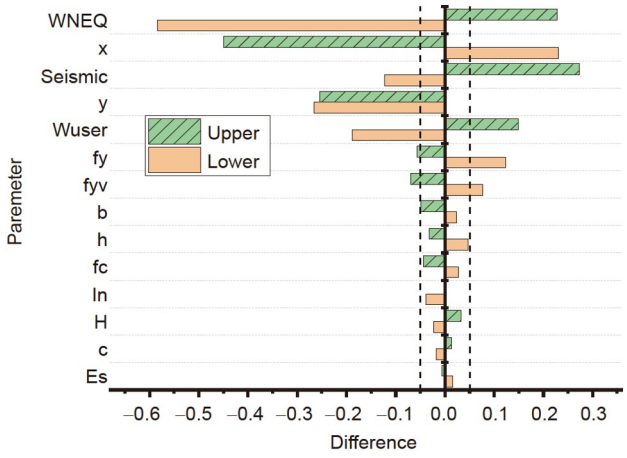

Figure 8 (Color online) Sensitivity analysis tornado chart.

streamlining the calculation, the variability of the above variables with less impact will not be considered subsequently and their average values will be considered as the actual values in the calculation for subsequent modeling and calculation.

4.3 Analysis of damage probability of RC column under the combined seismic and blast loads

In this section, the damage probability of RC column members under combined seismic and blast loads is studied by Monte Carlo simulation method. The working conditions are seismic intensity 7, the nominal mass of explosive 1000 kg for VBIED explosion scenario, nominal mass of equivalent TNT mass Wnom is 607 kg, and the distance of explosion is 10 m. According to the above conditions, a sample set with capacity 100 is extracted using MATLAB software, and its variables are the parameters that need to be taken into consideration as screened by sensitivity analysis. The FEM model of RC column is established based on the sample set. And the seismic and explosion parameters in the sample set are used to perform the FEM analysis based on the restart function of LS-DYNA, which is subjected to the seismic action first and then to the explosion action. The results are compared with the working conditions subjected to the seismic action alone and the explosion action alone.

The cumulative distribution function (CDF) of the damage probability of the damage index D_s for the RC column under the earthquake disaster alone, the damage probability CDF of damage index D_b for the RC column under the explosion disaster alone, and the damage probability CDF of damage index D_m for the RC column under the earthquake disaster first and the explosion disaster later are shown in Figure 9. It can be seen that the damage probability of RC column after suffering an earthquake is less than suffering an explosion, while its damage probability after suffering an explosion is less than suffering two disasters successively. What's more, CDF function shape of D_m is similar to that of D_s, indicating

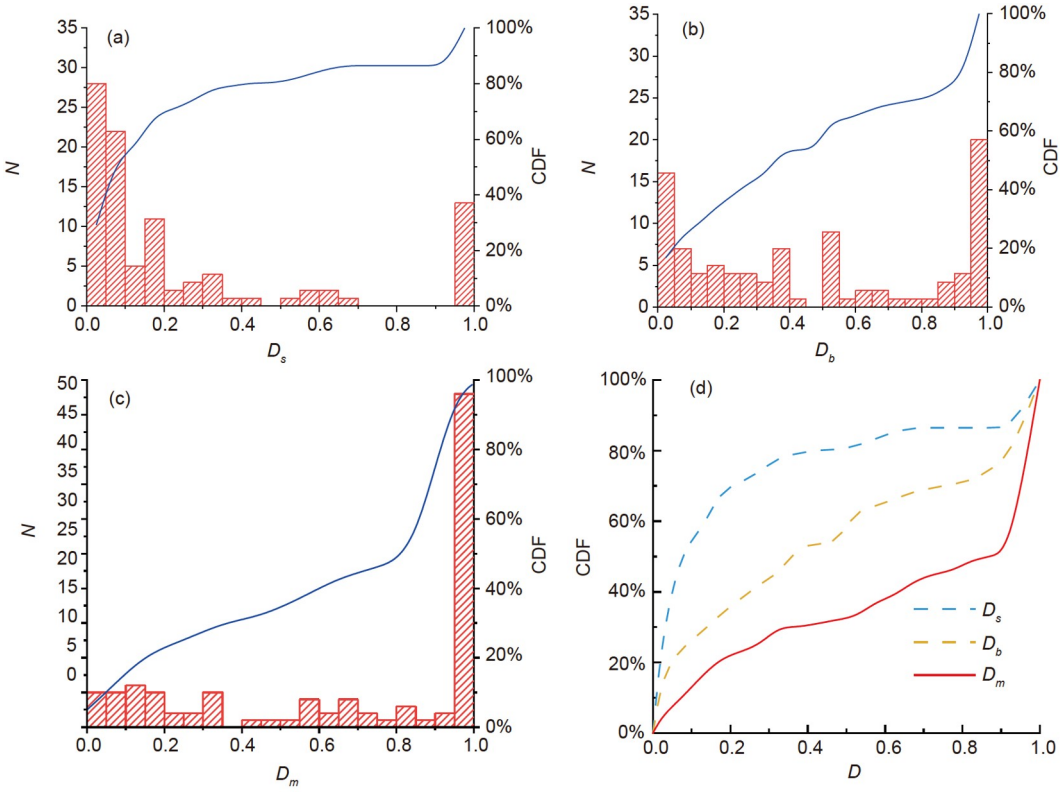

Figure 9 (Color online) Cumulative distribution function (CDF) of D_s, D_b, D_m. (a) D_s-CDF; (b) D_b-CDF; (c) D_m-CDF; (d) contrast chart.

that the blast effect is the main reason that causes the damage of the RC column. And the initial damage caused by the seismic load cannot be neglected because it will increase the damage probability of RC column.

In order to clarify the influence of different design parameters on the damage probability under the combined effect of seismic and blast hazards, six parameters were selected for the parametric analysis of the damage probability: column depth h, column width b, column height H, concrete strength f_c, hoop spacing s, and axial compression ratio n. The selected values are shown in Table 10.

The comparison of damage probability CDF of RC column with different values of parameters is shown in Figure 10. It can be seen that increasing the column width, column depth, and column height can reduce the damage probability of RC columns in case of seismic hazard, while decreasing the hoop spacing and the vertical axial compression ratio can reduce the damage probability in case of seismic hazard, and for concrete compressive strength, too large or too small compressive strength can lead to higher damage probability. This indicates that in the seismic design of RC columns, it is necessary to reduce the probability of damage in case of seismic hazard by selecting the appropriate stiffness to ensure the safety of the structure.

The comparison of the damage probability of RC column members under the blast hazard with different values of parameters is shown in Figure 11. It can be seen that increasing the column width, decreasing the column depth and column height can better reduce the damage probability of RC columns under blast hazard, while reducing the spacing of hoop reinforcement and increasing the compressive strength of concrete can reduce the damage probability under seismic hazard, and for the vertical axial pressure ratio, selecting a moderate axial pressure ratio can minimize the damage probability.

Table 10 The values of the parameters control group and test group are taken

Parameters	Control group	Experimental group		
h (mm)	400	500	600	
b (mm)	400	500	600	
H (mm)	3600	3200	4000	
f_c (MPa)	40	30	50	
s (mm)	200	150	100	
n	0.2	0.1	0.3	0.4

The comparative damage probability of RC column members under joint action for different values of parameters is shown in Figure 12. It can be seen that increasing the column width and decreasing the column depth can significantly reduce the damage probability of RC columns under joint action and ensure the safety of the structure. At the same time, an axial pressure ratio larger than 0.3 will further aggravate the damage, leading to an increase in the probability of damage. The changes of column height, concrete compressive strength and hoop spacing have little

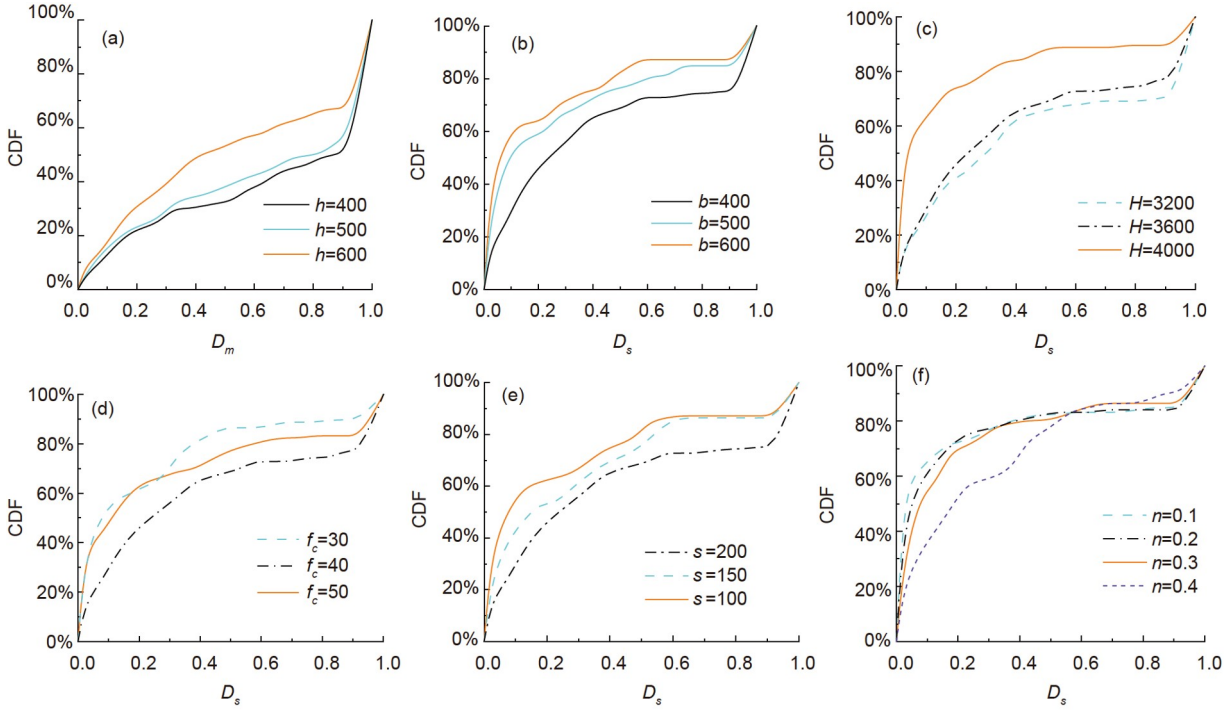

Figure 10 (Color online) Comparison of damage probability D_s-CDF for different values of parameters. (a) h; (b) b; (c) H; (d) f_c; (e) s; (f) n.

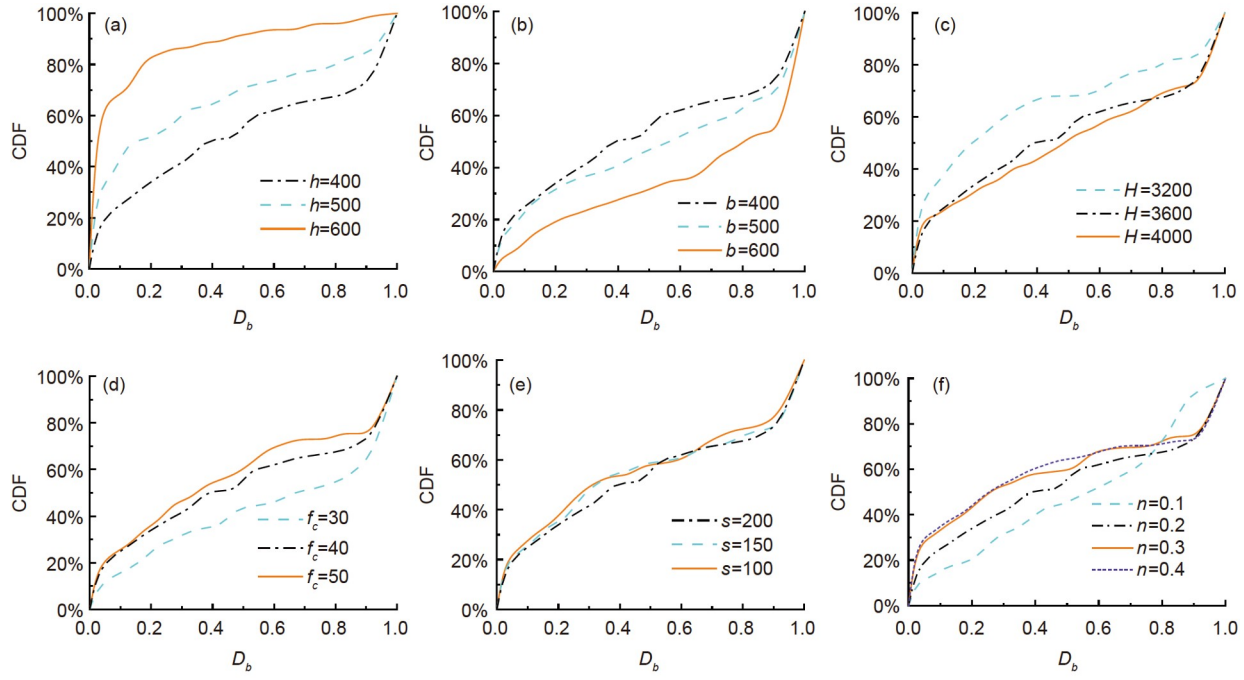

Figure 11 (Color online) Comparison of damage probability D_b-CDF for different values of parameters. (a) h; (b) b; (c) H; (d) f_c; (e) s; (f) n.

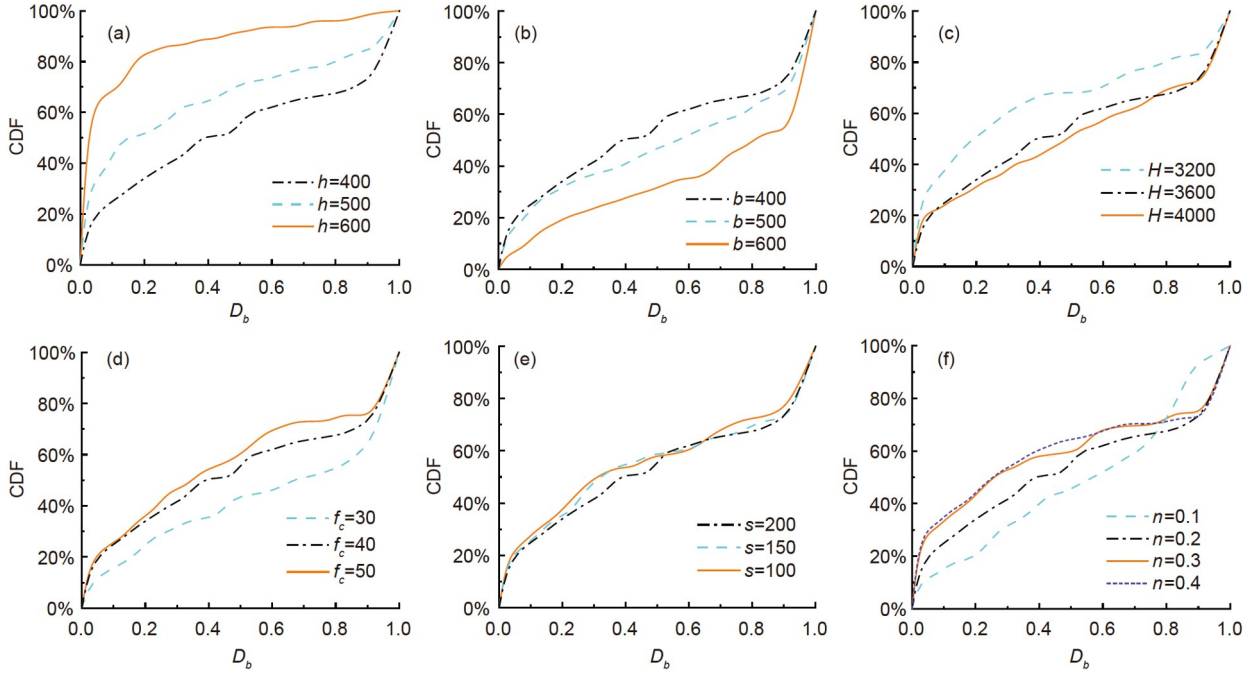

Figure 12 (Color online) Comparison of damage probability D_m-CDF for different values of parameters. (a) h; (b) b; (c) H; (d) f_c; (e) s; (f) n.

effect on the increase or decrease of damage probability. It can be seen that the design of protection for structures under joint action should be different from the design of protection under consideration of separate hazards, where a design favorable at the time of earthquake hazard or explosion hazard design may instead lead to unfavorable effects at multi-hazards.

4.4 Damage classification of RC column under the combined effect of earthquake and explosion

When considering the damage classification problem of

combined earthquake and explosion action, we need a classification criterion that can effectively determine the damage under the combined action. According to the calculation results of Monte Carlo method, three residual bearing capacity coefficients are counted and analyzed, and the two single-hazard results D_s and D_b are plotted in the plane diagram as x-coordinates and y-coordinates, respectively, and their multi-hazard damage D_m is used as the basis for classification. The sample set results were classified into three sets of failure (D_m>0.8), general damage (0.2<D_m<0.8), and undamaged (D_m<0.2), and the classification results for the sample set are shown in Figure 13.

It can be observed that the boundary between different groupings is more obvious, so the damage under multi-hazards can be discerned after clarifying the boundary line between different groupings. To accurately and conveniently find the analytic form of grouping boundaries, statistical analysis of grouping boundaries can be performed using the SVM algorithm, also known as the support vector machine algorithm to solve the problem of identifying machine learning in small-sample, nonlinear and high-dimensional pattern recognition, which can obtain the best generalization capability and accuracy based on limited sample information. For a training set $D(x, y)$ with the number of items n, it can be grouped accurately according to eq. (20).

$$f(x)=\operatorname{sgn}\left\{\left[\sum_{j=1}^{l}\alpha_j^* y_i(x_j+x_i)\right]+b^*\right\}. \tag{20}$$

Now we use MATLAB based on SVM algorithm to solve the set boundary with different damage degrees under multi-hazards and simplify it to a linear boundary, whose dividing line is shown in Figure 14.

In Figure 14, the boundary equation between the general damage set and the undamaged set is determined by eq. (21).

$$\left(\frac{D_s}{0.390}\right)^{1/2}+\left(\frac{D_b}{0.259}\right)^{1/2}=1. \tag{21}$$

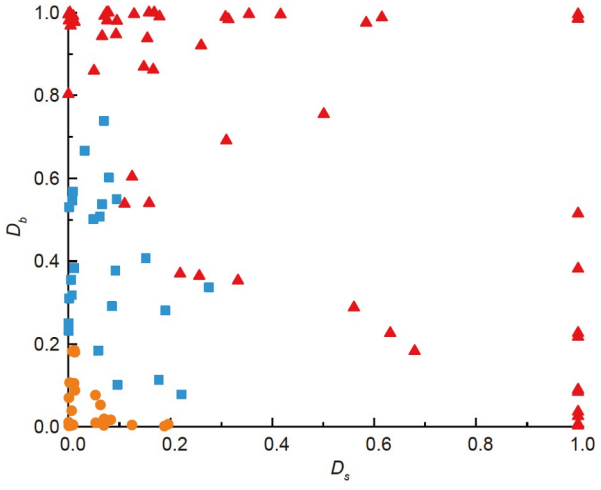

Figure 13 (Color online) Relationship and grouping of D_s and D_b.

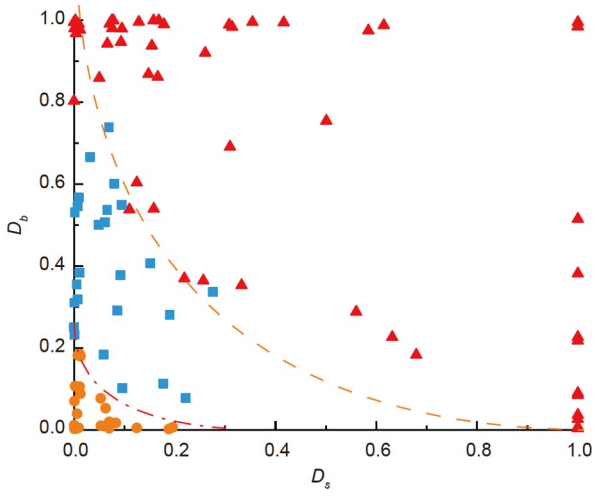

Figure 14 (Color online) Corresponding grouping and demarcation line of D_s and D_b.

The boundary equation between the failure set and the general damage set is determined by eq. (22).

$$\left(\frac{D_s}{1.035}\right)^{1/2}+\left(\frac{D_b}{1.259}\right)^{1/2}=1. \tag{22}$$

Therefore, for the combined action of the earthquake and explosion to discriminate the boundary of the form of the dividing line, set the general form of the dividing line as in eqs. (23) and (24). Where the general damage collection and undamaged collection of the dividing line fitting formula is determined by eq. (23), the general damage collection and failure collection of the dividing line fitting formula is determined by eq. (24). As in the previous section, the six parameters of Table 10 were selected for the parametric analysis, and the partition images of the residual bearing capacity coefficients under combined earthquake and blast are shown in Figure 15.

$$\left(\frac{D_s}{s_{0,\mathrm{I}}}\right)^{1/2}+\left(\frac{D_b}{b_{0,\mathrm{I}}}\right)^{1/2}=1, \tag{23}$$

$$\left(\frac{D_s}{s_{0,\mathrm{II}}}\right)^{1/2}+\left(\frac{D_b}{b_{0,\mathrm{II}}}\right)^{1/2}=1. \tag{24}$$

The formulas obtained by fitting the analytic formulas of each divider in Figure 15, while fitting the four parameters in the form of eqs. (23) and (24) are shown in eqs. (25)–(28). The empirical equations are only applicable to RC columns within the ranges of parametric studies. Accordingly, the analytical equation of the dividing line for rapid classification of the damage level under the combined action of earthquake and explosion can be obtained for RC columns under combined seismic and blast loads. Firstly, the damage index of the RC column under a single seismic load or blast load should be defined separately, i.e., D_s and D_b. Then the range of damage degree can be obtained in the D_s-D_b curve according to the location of the (D_s, D_b) point, and the

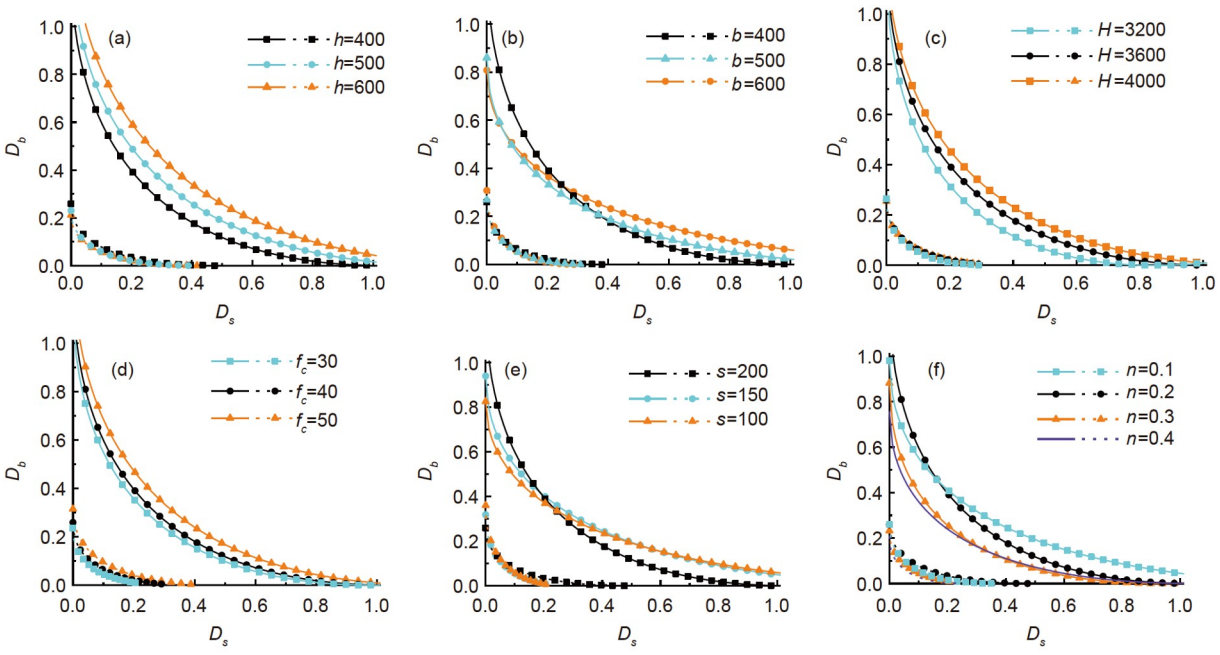

Figure 15 (Color online) Comparison of cut-offs at different parameter values. (a) h; (b) b; (c) H; (d) f_c; (e) s; (f) n.

damage degree of RC column under the combined seismic and blast loads can be roughly obtained, that is, mild, moderate or failure.

$$s_{0,\mathrm{I}} = 0.269 \times \ln\left(\frac{h}{400}\right) - 0.077 \times \ln\left(\frac{b}{400}\right) - 0.241 \times \ln\left(\frac{H}{3600}\right) + 0.291 \times \ln\left(\frac{f_c}{40}\right) + 8.515 \times \ln\left(\frac{s}{200}\right) - 8.487 \times \ln\left(\frac{n}{0.2}\right) + 0.330, \quad (25)$$

$$b_{0,\mathrm{I}} = -0.157 \times \ln\left(\frac{h}{400}\right) + 6.387 \times \ln\left(\frac{b}{400}\right) - 0.039 \times \ln\left(\frac{H}{3600}\right) + 0.152 \times \ln\left(\frac{f_c}{40}\right) - 0.132 \times \ln\left(\frac{s}{200}\right) - 0.110 \times \ln\left(\frac{n}{0.2}\right) + 0.272, \quad (26)$$

$$s_{0,\mathrm{II}} = 0.719 \times \ln\left(\frac{h}{400}\right) + 1.705 \times \ln\left(\frac{b}{400}\right) + 1.628 \times \ln\left(\frac{H}{3600}\right) - 0.418 \times \ln\left(\frac{f_c}{40}\right) - 1.160 \times \ln\left(\frac{s}{200}\right) - 0.425 \times \ln\left(\frac{n}{0.2}\right) + 1.141, \quad (27)$$

$$b_{0,\mathrm{II}} = 0.966 \times \ln\left(\frac{h}{400}\right) - 0.873 \times \ln\left(\frac{b}{400}\right) - 0.408 \times \ln\left(\frac{H}{3600}\right) + 0.271 \times \ln\left(\frac{f_c}{40}\right) + 0.460 \times \ln\left(\frac{s}{200}\right) - 0.226 \times \ln\left(\frac{n}{0.2}\right) + 1.124. \quad (28)$$

5 Conclusions

In this study, using the explicit dynamic analysis finite element software LS-DYNA, the degree and probability of damage of RC column under combined seismic and blast loads were investigated, and the following main conclusions were obtained.

(1) The influence of the parameter variability of RC columns on the damage probability analysis was determined. It is found that the damage randomness of RC columns is more significantly affected by the degree of randomness of load parameters than by the randomness of geometric parameters and material parameters. Therefore, the uncertainties in load parameters should be considered in damage probability analysis of RC column under combined seismic and blast loads.

(2) The relationships between the damage degree of RC column under individual seismic or blast loads and their combination were analyzed and fitted. Monte Carlo method together with the SVM algorithm is used to determine the dividing line between different damage degree groups of RC column under combined seismic and blast loads. An empirical formulation to determine the damage degree of RC columns under the combined seismic and blast loads is proposed.

(3) The recommendations for design of RC column against multi-hazard are put forward. Increasing column depth, hoop spacing, and concrete strength can effectively improve the resistance of RC column to multi-hazard.

This work was supported by the National Natural Science Foundation of

China (Grant Nos. 51878445, 51938011 and 51908405).

1 Li Y, Ahuja A, Padgett J E. Review of methods to assess, design for, and mitigate multiple hazards. J Perform Constr Facil, 2012, 26: 104–117
2 Fascetti A, Kunnath S K, Nisticò N. Robustness evaluation of RC frame buildings to progressive collapse. Eng Struct, 2015, 86: 242–249
3 Lin K, Lu X, Li Y, et al. Experimental study of a novel multi-hazard resistant prefabricated concrete frame structure. Soil Dyn Earthq Eng, 2019, 119: 390–407
4 Abdollahzadeh G, Faghihmaleki H. Seismic-explosion risk-based robustness index of structures. Int J Damage Mech, 2017, 26: 523–540
5 Faghihmaleki H. A plastic design method for RC moment frame buildings against progressive collapse. Makara J Technol, 2017, 21: 7
6 Abdollahzadeh G, Faghihmaleki H. Probabilistic two-hazard risk assessment of near-fault and far-fault earthquakes in a structure subjected to earthquake-induced gas explosion. J Build Eng, 2017, 13: 298–304
7 Abdollahzadeh G, Faghihmaleki H. Proposal of a probabilistic assessment of structural collapse concomitantly subject to earthquake and gas explosion. Front Struct Civ Eng, 2018, 12: 425–437
8 Feng D C, Xie S C, Xu J, et al. Robustness quantification of reinforced concrete structures subjected to progressive collapse via the probability density evolution method. Eng Struct, 2020, 202: 109877
9 Stochino F, Attoli A, Concu G. Fragility curves for RC structure under blast load considering the influence of seismic demand. Appl Sci, 2020, 10: 445
10 Elhami Khorasani N, Garlock M, Gardoni P. Probabilistic performance-based evaluation of a tall steel moment resisting frame under post-earthquake fires. J Struct Fire Eng, 2016, 7: 193–216
11 Tu Z, Lu Y. Evaluation of typical concrete material models used in hydrocodes for high dynamic response simulations. Int J Impact Eng, 2009, 36: 132–146
12 Hallquist J. LS-DYNA Keyword User's Manual. Version: 970. Livermore: Livermore Software Technology Corporation, 2003
13 Malvar L J, Crawford J E, Wesevich J W, et al. A plasticity concrete material model for DYNA3D. Int J Impact Eng, 1997, 19: 847–873
14 Malvar L J, Ross C A. Review of strain rate effects for concrete in tension. ACI Mater J, 1998, 95: 735–739
15 Bischoff P H, Perry S H. Compressive behaviour of concrete at high strain rates. Mater Struct, 1991, 24: 425–450
16 Comité Euro-International du Béton. CEB-FIP Model Code 1990: Design Code. London: Thomas Telford Publishing, 1993
17 Javier Malvar L, Crawford J E. Dynamic Increase Factors for concrete. In: Twenty-Eighth DDESB Seminar. Orlando, 1998
18 Mamalis A G, Manolakos D E, Ioannidis M B, et al. Static axial collapse of foam-filled steel thin-walled rectangular tubes: Experimental and numerical simulation. Int J Crashworthiness, 2008, 13: 117–126
19 Liu B, Villavicencio R, Guedes Soares C. Experimental and numerical plastic response and failure of pre-notched transversely impacted beams. Int J Mech Sci, 2013, 77: 314–332
20 Liu B, Villavicencio R, Guedes Soares C. On the failure criterion of aluminum and steel plates subjected to low-velocity impact by a spherical indenter. Int J Mech Sci, 2014, 80: 1–15
21 Ngo T, Mohotti D, Remennikov A, et al. Numerical simulations of response of tubular steel beams to close-range explosions. J Constr Steel Res, 2015, 105: 151–163
22 Qiu F, Pan P. Quasi-static loading and control for structural test (in Chinese). China Civil Eng J, 2002, 35: 1–5,10
23 US Department of Defense. Unified facilities criteria (UFC): Structures to resist the effects of accidental explosions. UFC-3-340-02. 2008
24 US Department of the Army, Navy and the Air Force. Structures to resist the effect of accidental explosions. TM5-1300. 1990
25 Emergency Management Agency (FEMA). Reference manual to minigate potenial terrorist attacks against buildings. FEMA-426, 2003
26 Woodson S C, Baylot J T. Structural Collapse: Quarter-Scale Model Experiments. Army Engineer Waterways Experiment Station Vicksburg MS Structures Lab., 1999
27 Woodson S C, Baylot J T. Quarter-scale building/column experiments. In: Structures Congress. Philadelphia, 2000
28 Netherton M D, Stewart M G. Blast load variability and accuracy of blast load prediction models. Int J Protect Struct, 2010, 1: 543–570
29 Wiśniewski D F, Cruz P J S, Henriques A A R, et al. Probabilistic models for mechanical properties of concrete, reinforcing steel and pre-stressing steel. Struct Infrastr Eng, 2012, 8: 111–123
30 Lee T H, Mosalam K M. Probabilistic fiber element modeling of reinforced concrete structures. Comput Struct, 2004, 82: 2285–2299
31 Hao H, Stewart M G, Li Z X, et al. RC column failure probabilities to blast loads. Int J Protective Struct, 2010, 1: 571–591